

Supporting Information

Cyanine-Based Nanoparticles for Near-Infrared Triggered Photothermal Therapy against *S. aureus*

Shuang Song^{1,2}, Na Yang^{2,3}, Di He^{2,3}, Ying Li^{*2,3}, Mahmood Hassan Akhtar^{2,3}, Chang
Liu^{2,3}, Xiwen Li^{2,3}, Xiande Shen^{*1,4} and Cong Yu^{*2,3}

¹ *College of Materials Science and Engineering, School of Materials Science and Engineering, Changchun University of Science and Technology, Changchun, 130022, China*

² *State Key Laboratory of Electroanalytical Chemistry, Changchun Institute of Applied Chemistry, Chinese Academy of Sciences, Changchun 130022, China*

³ *School of Applied Chemistry and Engineering, University of Science and Technology of China, Hefei 230026, China*

⁴ *Chongqing Research Institute, Changchun University of Science and Technology, No. 618 Liangjiang Avenue, Longxing Town, Yubei District, Chongqing City 401135, China*

Author E-mails: liying666@ciac.ac.cn (Y. Li); shenxiande@cust.edu.cn (X.D. Shen); congyu@ciac.ac.cn (C. Yu).

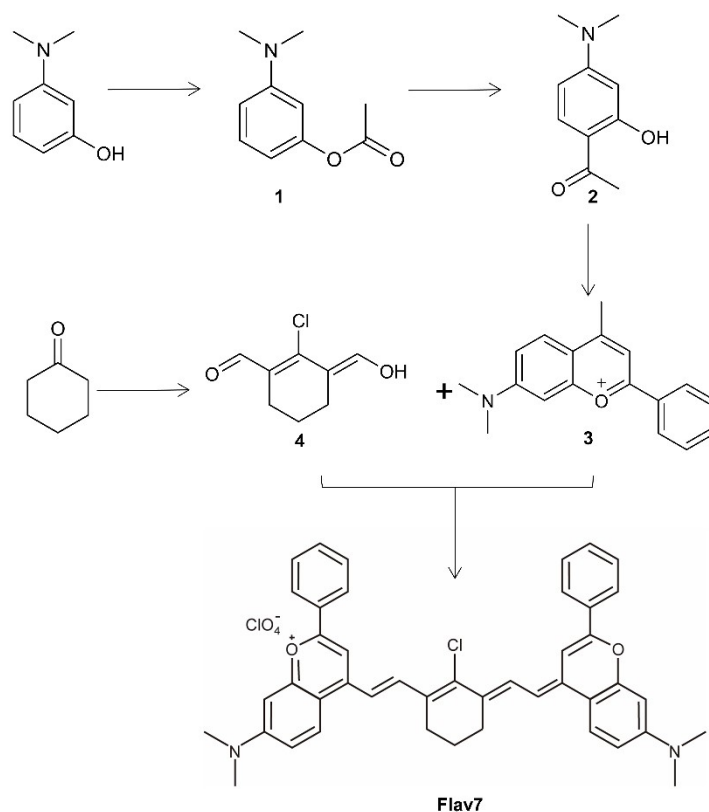
1. Apparatus

¹H-NMR spectra were obtained by a Bruker 500 MHz spectrometer. Mass spectra were recorded by a Bruker Mass spectrometer (Bruker Daltonic flex analysis). UV-Vis-NIR absorption spectra were recorded with a Cary 50 Bio Spectrophotometer (Varian Inc., CA, USA) equipped with a xenon flash lamp. Cell viability data were recorded by a Synergy microplate reader (BioTek, USA). Transmission electron microscopy (TEM) measurements were performed on a FEI TECNAI G2 high resolution transmission electron microscope (the Netherlands). An infrared thermal

imaging camera and an 808 nm NIR laser (1.0 W/cm²) were used to monitor images of the photothermal effects in the presence of the NPs.

2. synthetic route of Flav7

The detailed synthetic route of Flav7 is described in **Scheme S1**. The procedures followed previously reports with some small adjustments^{1,2}.



Scheme S1. Synthetic route of Flav7.

Compound 1: 3-dimethylaminophenol (0.69 g, 5 mmol, 1.0 eq), and triethylamine (0.84 mL, 6 mmol, 1.2 eq) were dissolved in DCM and stirred in an ice bath for 10 min under nitrogen atmosphere. Then acetyl chloride (0.39 mL, 5.5 mmol, 1.1 eq) in DCM was added via a constant pressure dropping funnel. Later, the reaction mixture was cooled to room temperature and stirred for another 12 h. After being quenched

with water, the aqueous phase was extracted with DCM. The DCM solution was collected, washed with saturated salt water, and dried over anhydrous sodium sulfate. Solvent was removed by vacuum-rotary evaporation to obtain a dark red liquid (0.85 g, 96% yield). ¹H NMR (500 MHz, CDCl₃): δ (ppm) 7.21 (m, 1H), 6.62 (d, *J* = 8.0 Hz, 1H), 6.45 (m, 2H), 2.94 (s, 6H), 2.29 (s, 3H).

Compound 2: Compound 1 (0.72 g, 4.0 mmol, 1 eq), NaCl (0.24 g, 4.0 mmol, 1 eq) and AlCl₃ (1.6 g, 12.0 mmol, 3 eq) were added in flask and refluxed at 80 °C for 3 h. Temperature of the reaction mixture was increased to 140 °C for another 6 h. The reaction was quenched by slowly adding 1 M HCl (20 mL), and the mixture was extracted with DCM. After solvent removal, the raw product was purified using column chromatography (gradient elution from PE to PE/EA = 10/1) to get white crystals (0.325 g, 44.8% yield). ¹H NMR (500 MHz, CDCl₃): δ (ppm) 12.88 (s, 1H), 7.54 (d, *J* = 9.0 Hz, 1H), 6.23 (dd, *J* = 9.0 Hz, 2.5 Hz, 1H), 6.11 (d, *J* = 2.5 Hz, 1H), 3.05 (s, 6H), 2.50 (s, 3H).

Compound 3: Compound 2 (0.18 g, 1.0 mmol, 1 eq) and acetophenone (0.12 g, 1.0 mmol, 1.0 eq) were dissolved in CH₃COOH (7.2 mL), and HClO₄ (3.5 mL) was added dropwise at room temperature. The reaction temperature was increased to 60 °C and kept for 6 h, and to 130 °C and kept for another 13 h. After being cooled to room temperature, 100 mL of water was poured in to facilitate precipitation of the red product. The precipitate was filtered, washed with EA, and dried under vacuum to

obtain compound 3 without further purification (0.28 g, 80% yield). ¹H NMR (500 MHz, D₂O): δ (ppm) 8.26–8.23 (m, 2H), 8.13 (d, *J* = 10.0 Hz, 1H), 7.93 (s, 1H) 7.59–7.67 (m, 3H), 7.44 (dd, *J* = 10.0 Hz, 2.5 Hz, 1H), 7.18 (d, *J* = 2.5 Hz, 1H), 3.32 (s, 6H), 2.85 (s, 3H).

Compound 4: 5 mL DMF was mixed with 5 mL DCM and stirred on an ice bath, a solution of 3.5 mL POCl₃ in 5 mL DCM was added dropwise. After 30 min, cyclohexanone was added (1.0 g, 10.2 mmol, 1 eq), the resulting mixture was refluxed with vigorous stirring for 4 h at 80 °C, which was subsequently poured into ice-cold water, and left overnight to obtain compound 4 as a yellow solid (1.39 g, 78%) after filtration and drying. ¹H NMR (500 MHz, CDCl₃): δ (ppm) 8.83 (s, 1H), 2.47 (t, *J* = 6.0 Hz, 4H), 1.71 (m, 2H).

Flav7: A solution of compound 3 (1.0 g, 2.8 mmol, 1.7 eq) and compound 4 (283 mg, 1.6 mmol, 1.0 eq) in a mixed solvent of *n*-butanol (20 mL) and benzene (10 mL) was stirred at 110 °C for 10 h under nitrogen atmosphere. After being cooled to room temperature, solvent was evaporated under reduced pressure and the crude product was washed with a small amount of DCM. Flav7 was purified by column chromatography (gradient elution from DCM to DCM/MeOH = 10/1) to get Flav7 as a dark purple solid (58 mg, 56% yield). ¹H NMR (500 MHz, DMSO-*d*₆): δ (ppm) 8.16 (d, *J* = 15.0 Hz, 2H), 8.08- 8.04 (m, 6H), 7.56 (m, 8H), 6.99 (d, *J* = 10.0 Hz, 2H), 6.91 (dd, *J* = 10.0 Hz, 2.5 Hz, 2H), 6.73 (d, *J* = 2.5 Hz, 2H), 3.12 (s, 12H), 2.79 (m,

4H), 1.89 (t, $J = 6.3$ Hz, 2H). MS (MALDI): Calc. for $C_{44}H_{40}N_2O_2Cl^+$, 663.28; Found: 663.3.

3. Characterization of the Flav7@DSPE-PEGG NPs

UV-vis absorption spectra of Flav7 and the Flav7@DSPE-PEGG NPs were recorded on a Cary 50 Bio Spectrophotometer. Morphology and size of the Flav7@DSPE-PEGG NPs were measured by transmission electron microscopy (TEM) and dynamic light scattering (DLS), respectively. Zeta potential measurements were employed to get the surface potential value of the Flav7@DSPE-PEGG NPs.

4. Photothermal conversion efficiency of the Flav7@DSPE-PEGG NPs

According to previous literature,³ sample solutions (1.315 g) of the Flav7@DSPE-PEGG NPs ($A_{808nm}=0.74$) and water (1.315 g) were irradiated with 808 nm laser at 1.0 W/cm² for 10 min and cooled to ambient temperature, and the subsequent temperature changes were recorded. The calculated the photothermal conversion efficiency was 37.21%.

5. Bacterial culture

S. aureus, *E. coli*, and *P. aeruginosa* were cultured in LB liquid broth medium under shaking (150 rpm) at 37 °C for 14 h, washed and then suspended in PBS. Optical density (OD) at 600 nm was measured with a UV-vis spectrometer. Following the OD₆₀₀ value, bacterial suspensions (1×10^8 CFU/mL) were prepared and directly used

in subsequent experiments.

6. In vitro evaluation of antibacterial activity of the Flav7@DSPE-PEGG NPs

S. aureus suspension (1×10^8 CFU/mL) was mixed with different concentrations of the Flav7@DSPE-PEGG NPs (0, 10, 15, 20 μ M) in a 96-well plate (total volume: 300 μ L). Then, the assay mixtures were incubated at 37 °C for 15 min and irradiated with 808 nm NIR laser (1.0 W/cm²) for 10 min. After that, each sample solution was diluted 10000 times with PBS, and 100 μ L of the diluted solution was spread on an LB agar plate. After incubation for 24 h, bacterial colonies of the control group and the experimental group were counted and recorded by *image J*. Antibacterial performance was calculated using the following equation:

$$\text{Survival ratio (\%)} = \text{CFU (sample)}/\text{CFU (control)} \times 100\%$$

7. Observation of Bacterial Morphology Destruction

S. aureus was incubated with PBS (the control group) or the NPs (20 μ M) for 30 min, and then exposed to 808 nm laser for 10 min. The bacteria were washed and centrifuged several times. The collected bacteria were then fixed in 2.5% glutaraldehyde at 4 °C overnight. Finally, the bacteria were dehydrated with different concentrations of ethanol (30%, 50%, 70%, 90% and 100%). The morphology changes of bacteria were surveyed with a scanning electron microscope.

8. Hemolysis assay

After collection of fresh blood from BALB/C mice, red blood cells (RBCs) were centrifuged and washed three times in PBS at 2500 rpm for 15 minutes, and then diluted to 5% (v/v) and used for subsequent analysis. Different concentrations of the NPs (60, 80, and 100 μ M, PBS, water) were incubated with the RBCs at 37 $^{\circ}$ C for two hours. Water was selected as the positive control. PBS was used as the negative control. After centrifugation (2500 rpm, 15 min), 200 μ L aliquots were taken from the supernatant and transferred into a 96-well plate, and the absorbance (A) of hemoglobin released at 540 nm was measured using a Synergy microplate reader.

Hemolysis ratio was calculated according to the following equation:

$$\text{Hemolysis ratio (\%)} = (A_{\text{sample}} - A_{\text{negative}})/(A_{\text{positive}} - A_{\text{negative}}) \times 100\%$$

9. Cytotoxicity

Cell viability in the presence of the nanoparticles was evaluated by the traditional CCK-8 assay. L929 cells were planted in a 96-well plate (200 μ L 1640 in each plate, the cell density was about 5×10^4 cells/mL) and grown overnight in an incubator. Various amounts of the Flav7@DSPE-PEGG NPs were added and the samples were incubated for an additional 6 h. The culture medium was removed and 100 μ L of the fresh culture medium (containing 10% CCK-8) was added. The cells were further incubated for 3 h, and the absorption at 450 nm was recorded by a microplate reader.

Cell viability was calculated by the following equation:

$$\text{cell viability (\%)} = A_{\text{treatment}}/A_{\text{control}} \times 100\%$$

The control group: cells were incubated for 6 h with the culture medium without

addition of the NPs.

10. Evaluation of antibacterial activity of the Flav7@DSPE-PEGG NPs

The animal experiments were approved by the Animal Welfare and Ethics Committee of Changchun Institute of Applied Chemistry, Chinese Academy of Sciences, and carried out according to the NIH guidelines for the care and use of laboratory animals (NIH publication No. 85-23 Rev. 1985).

BALB/C mice (weight: 21-23 g) were first anesthetized with 1.25% tribromoethanol, and dorsal hair was shaved. Full-thickness cutaneous wounds (7 mm in diameter) were created following established procedures⁴. After wound formation, *S. aureus* suspension (1×10^9 CFU/mL, 20 μ L) was inoculated over each wound, and the bacterial infected injury model was constructed. After 18 h, the bacteria infected mice were randomly divided into three groups (n = 5) as follows: (i) PBS Group: 30 μ L PBS was inoculated to the wound tissue; (ii) “NPs” Group: 30 μ L Flav7@DSPE-PEGG NPs (40 μ M) was inoculated; (iii) “NPs + NIR” Group: 30 μ L Flav7@DSPE-PEGG NPs (40 μ M) was inoculated, after 15 min, the wound tissue was irradiated with 808 nm NIR laser (1.0 W/cm²) for 10 min. On day 10, the wound and surrounding tissues were harvested and fixed with 4% paraformaldehyde overnight and stained with hematoxylin and eosin (H & E), and Masson dye.

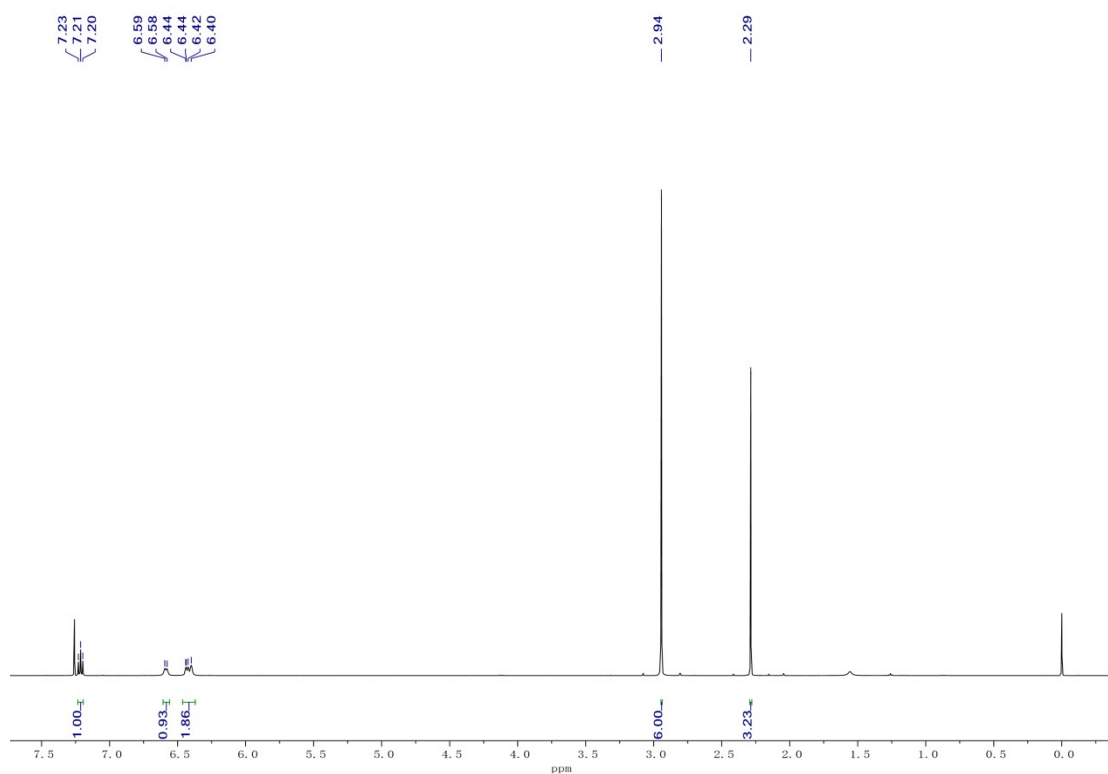


Fig. S1. ^1H NMR spectrum (500 MHz, CDCl_3 , room temperature) of compound 1.

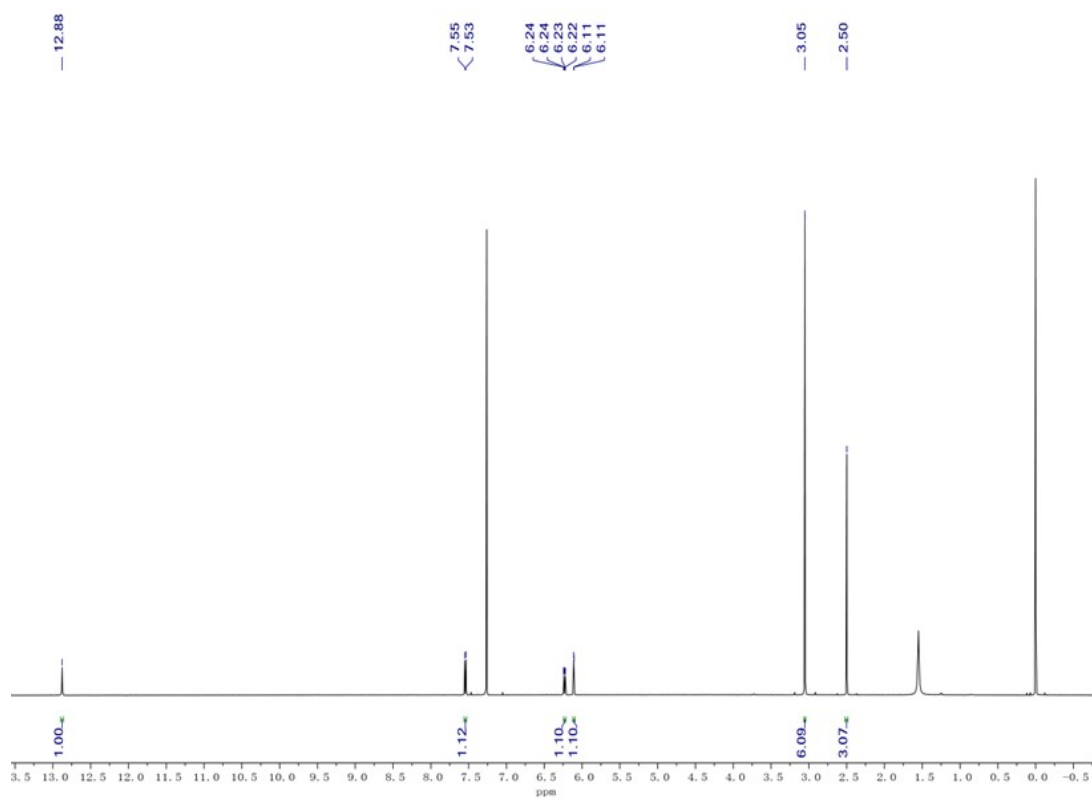


Fig. S2. ^1H NMR spectrum (500 MHz, CDCl_3 , room temperature) of compound 2.

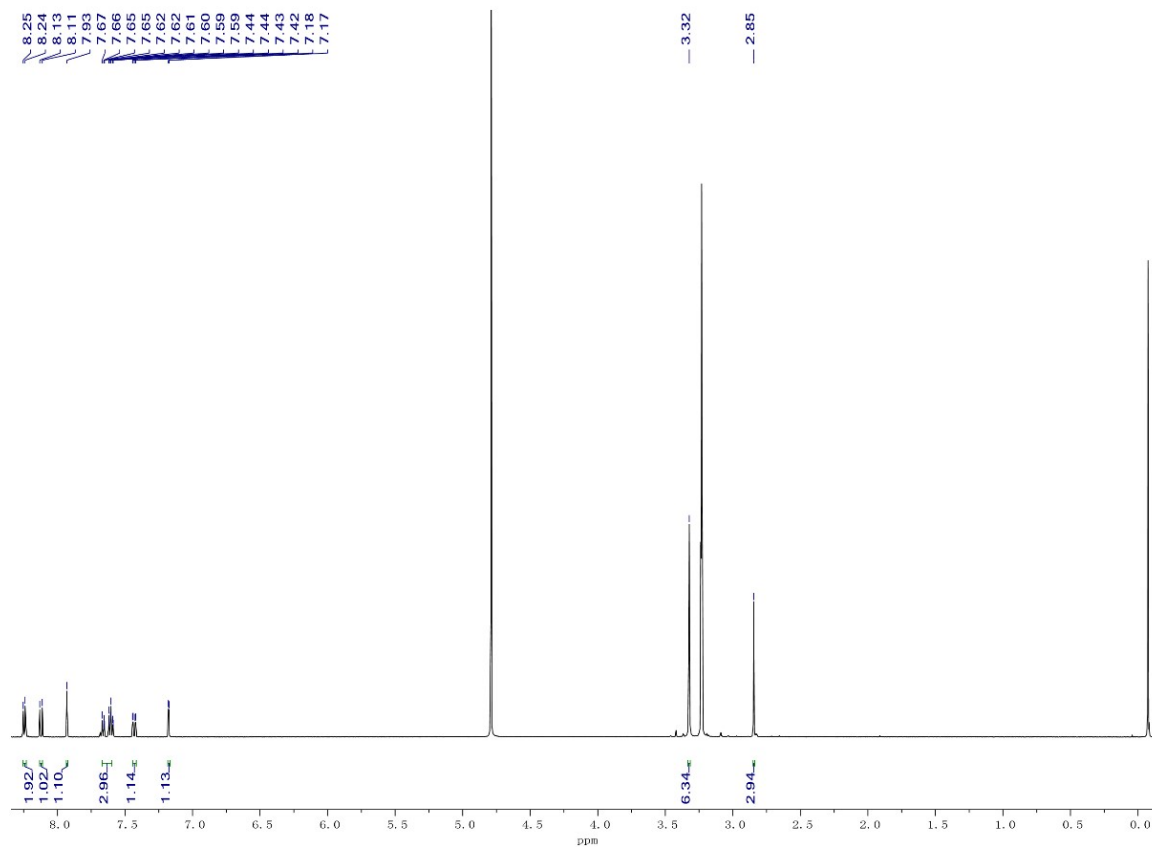


Fig. S3. ^1H NMR spectrum (500 MHz, D_2O , room temperature) of compound 3.

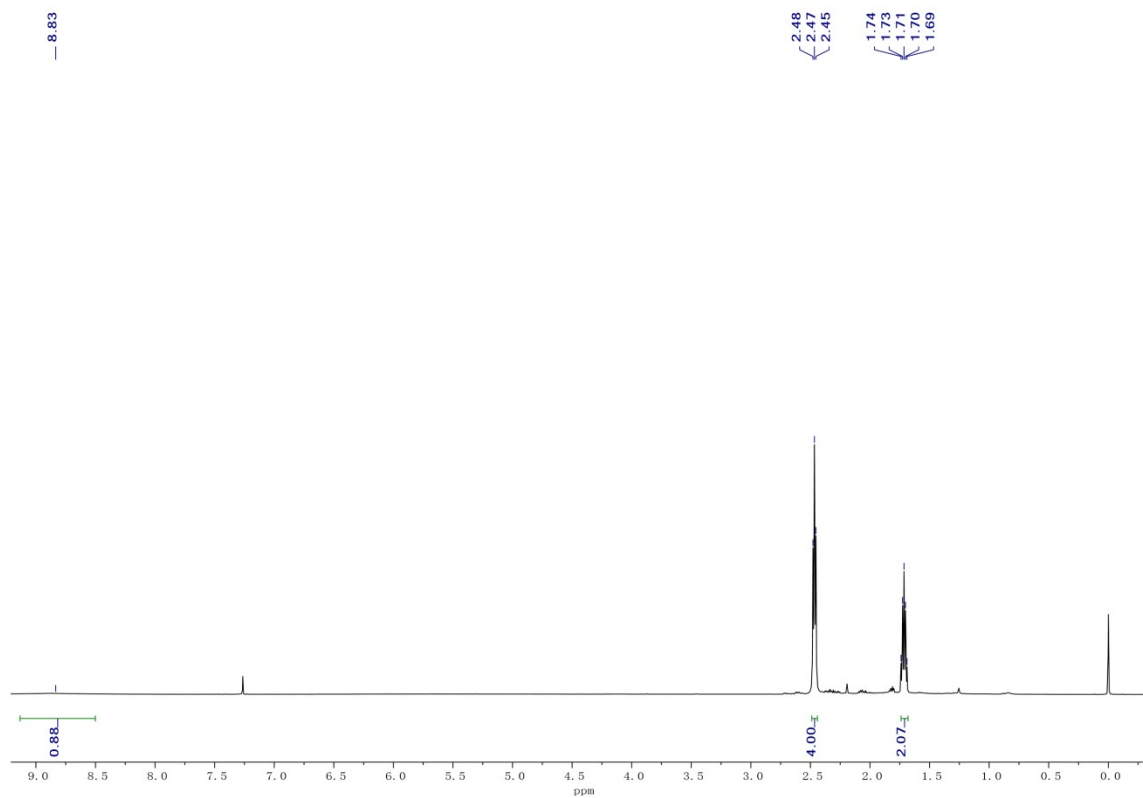


Fig. S4. ^1H NMR spectrum (500 MHz, CDCl_3 , room temperature) of compound 4.

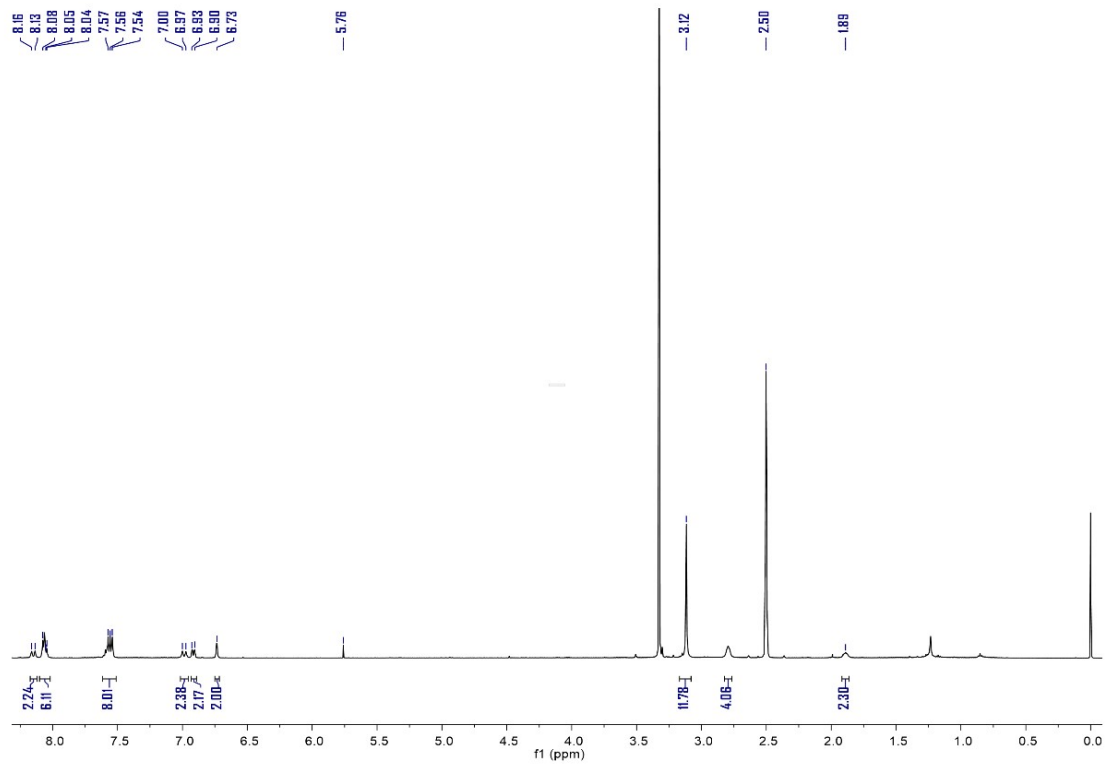
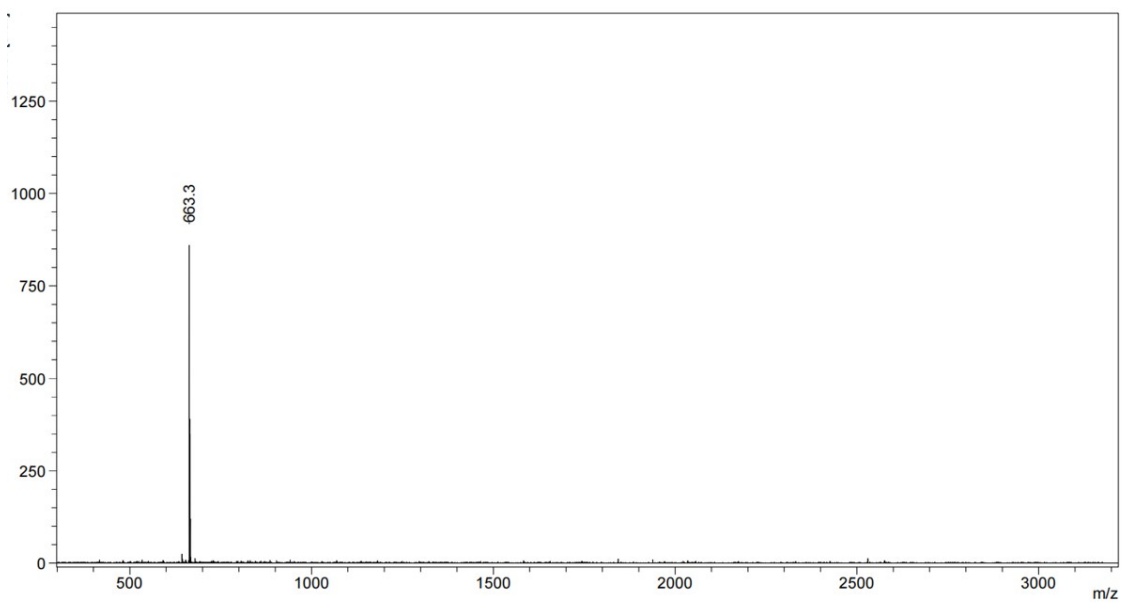


Fig. S5. ^1H NMR spectrum (500 MHz, $\text{DMSO-}d_6$, room temperature) of Flav7.

Fig. S6. MS analysis of Flav7 (CH_2Cl_2 , room temperature).



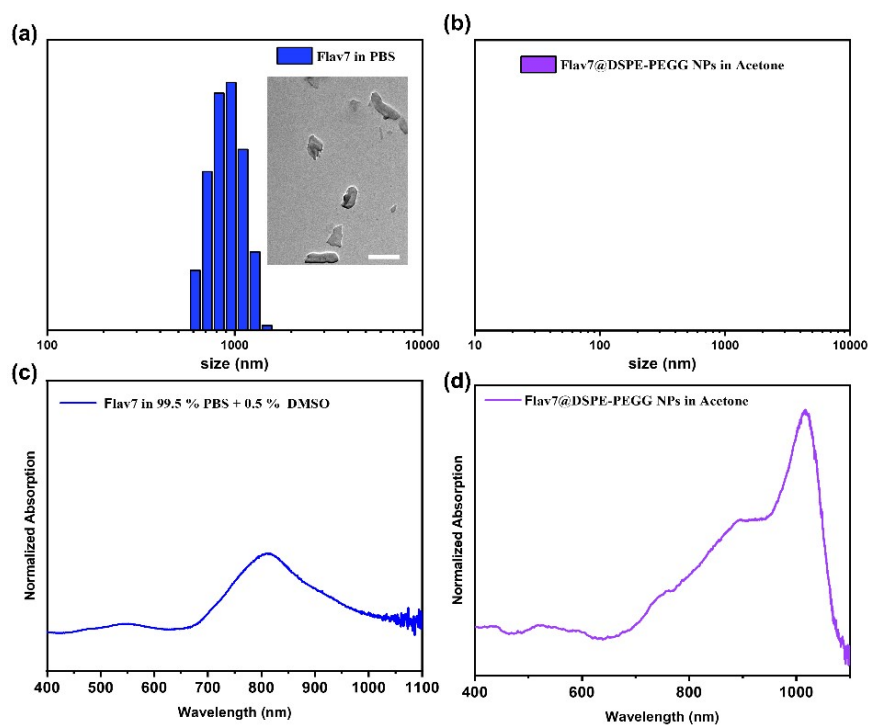


Fig. S7. (a) Fig. S7. (a) DLS size distribution and TEM image (inset) of Flav7 in PBS (scale bar: 1 μm). (b) DLS size distribution of the Flav7@DSPE-PEGG NPs in acetone. (c) Normalized UV-Vis-NIR spectra of Flav7 in 99.5 % PBS + 0.5 % DMSO. (d) Normalized UV-Vis-NIR spectra of the Flav7@DSPE-PEGG NPs in acetone.

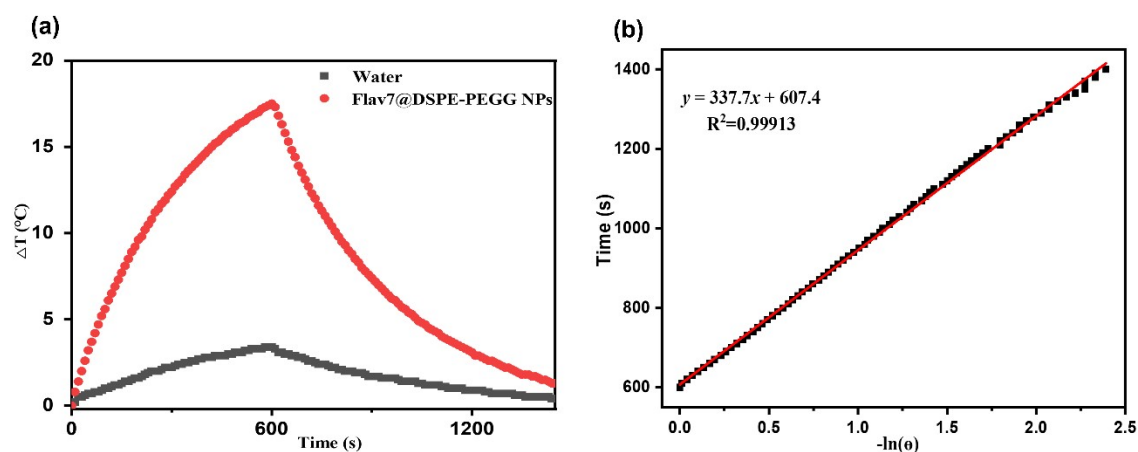


Fig. S8. Calculation of the photothermal conversion efficiency. (a) One on-off cycle.

(b) Linear curve of cooling time against the logarithm value of temperature.

Conditions: 808 nm laser, 1.0 W/cm².

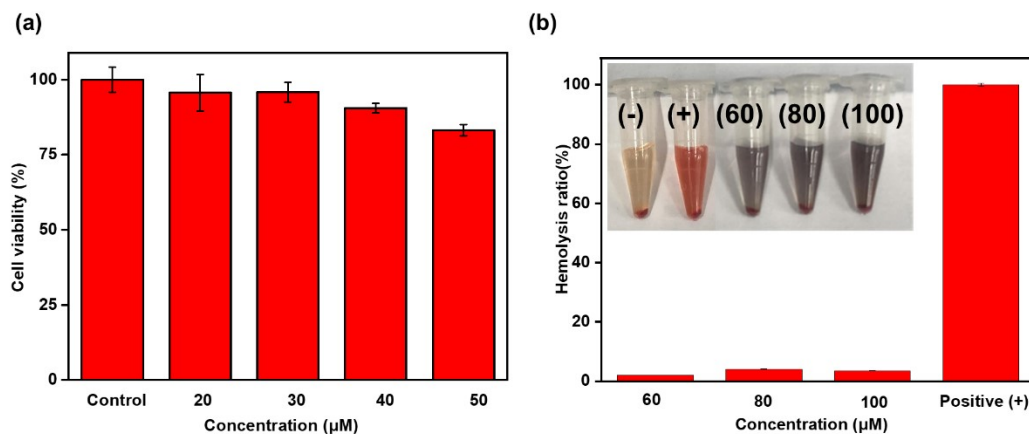


Fig. S9. (a) L929 cell viability when incubated with the Flav7@DSPE-PEGG NPs (50 μM) for 6 h. (b) Hemolysis ratio (%) of red blood cells incubated with different concentrations of the Flav7@DSPE-PEGG NPs (Inset: image of the red blood cell suspensions), (-): negative control (PBS), (+): positive control (water), nanoparticles concentration: 60, 80, 100 μM in PBS.

Table S1. Organic small molecule PTAs and their photothermal conversion efficiency.

Name	PTA	PCE	ref
NBDP NPs	aza-BODIPY	46%	5
CZ-Cy7	Cy7	77.5%	6
PXZ-Cy7		43.5%	
PTZ-Cy7		13%	
T780T	IR780	38.5%	7
Flav7@DSPE-PEGG NPs	Flav7	37.21%	Our work
BNPs	BODIPY	35.7%	8
DTZCy@SiO ₂ NPs	Cy7	34.6%	9
O-IDTBR NPs	O-IDTBR	33.7%	10
26NA-NIR/44BP-NIR	Cy7	35%	11
PY-AZB	aza-BODIPY	33%	12
TCPP NPs	Tetra (4-carboxy phenyl) porphyrin	31%	13
BODIPY-TPA NPs	BODIPY	20.7%	14
PEG-PTyr(¹²⁵ I)-ICG PMs	ICG	15.4%	15

References

1. E. D. Cosco, J. R. Caram, O. T. Bruns, D. Franke, R. A. Day, E. P. Farr, M. G. Bawendi and E. M. Sletten, *Angewandte Chemie International Edition*, 2017, **56**, 13126-13129.
2. T. Li, C. Li, Z. Ruan, P. Xu, X. Yang, P. Yuan, Q. Wang and L. Yan, *ACS Nano*, 2019, **13**, 3691-3702.
3. W. Zhen, Y. Liu, L. Lin, J. Bai, X. Jia, H. Tian and X. Jiang, *Angewandte Chemie International Edition*, 2018, **57**, 10309-10313.
4. S. Song, G. Xu, N. Yang, S. A. Shahzad, J. Lv, X. Shen and C. Yu, *Journal of Materials Science*, 2022, **57**, 21206-21218.
5. X. Ruan, M. Wei, X. He, L. Wang, D. Yang, Y. Cai, J. Shao and X. Dong, *Colloids and Surfaces B: Biointerfaces*, 2023, **231**, 113547.
6. J. Pan, J. Du, Q. Hu, Y. Liu, X. Zhang, X. Li, D. Zhou, Q. Yao, S. Long, J. Fan and X. Peng, *Advanced Healthcare Materials*, 2023, **12**, 2301091.
7. X. Zhao, H. Zhao, S. Wang, Z. Fan, Y. Ma, Y. Yin, W. Wang, R. Xi and M. Meng, *Journal of the American Chemical Society*, 2021, **143**, 20828-20836.
8. K. Liu, H. Liu, C. Li, Z. Xie and M. Zheng, *Biomaterials Science*, 2023, **11**, 195-207.
9. E. Feng, L. Jiao, S. Tang, M. Chen, S. Lv, D. Liu, J. Song, D. Zheng, X. Peng and F. Song, *Chemical Engineering Journal*, 2022, **432**, 134355.
10. C. Tang, Y. Pan, Z. Wei, L. Liu, J. Xu, W. Han and Y. Cai, *Colloids and Surfaces B: Biointerfaces*, 2024, **233**, 113611.
11. Y. Xu, J. Yu, J. Hu, K. Sun, W. Lu, F. Zeng, J. chen, M. liu, Z. Cai, X. He, W. Wei and B. Sun, *Advanced Healthcare Materials*, 2023, **12**, 2203080.
12. T. Pewklang, W. Saiyasombat, P. Chueakwon, B. Ouengwanarat, K. Chansaenpak, S. Kampaengsri, R.-Y. Lai and A. Kamkaew, *ChemBioChem*, 2023, **n/a**, e202300653.
13. B. Xu, Z. Wang and W. Zhao, *Dyes and Pigments*, 2021, **186**, 108926.
14. J. Deng, M. Yang, C. Li, G. Liu, Q. Sun, X. Luo and F. Wu, *Dyes and Pigments*, 2021, **187**, 109130.
15. L. Yang, C. Zhang, J. Liu, F. Huang, Y. Zhang, X.-J. Liang and J. Liu, *Advanced Healthcare Materials*, 2020, **9**, 1901616.